

**SIMULATION OF PC BEAM USING SFRC
BY CROSS SECTION ANALYSIS**

Hyeong Jae YOON, PhD, Arch.E., The Consulting Engineers Group, San Antonio, TX
M. Larbi SENNOUR, President, PhD, PE, SE, The Consulting Engineers Group,
San Antonio, TX

ABSTRACT

Steel-fiber reinforced concrete is increasingly being used day by day as a structural material, for example, coupling beam in the coupled shear wall structure. Steel-fiber reinforced concrete is expected to enhance the tensile properties of the resulting composite such as strength and stiffness. Many researchers have proposed evaluation methods of the flexural strength and material model of steel-fiber reinforced concrete members in the past. In addition, only a few researches have been conducted to examine the role of fibers in the area of prestressed concrete applications. In this study, an attempt has been made to evaluate the seismic behavior experimentally for prestressed concrete beams using steel-fiber reinforced concrete. Moreover, this study presents the results from a cross section analysis for one normal prestressed concrete beams and two prestressed concrete beams using steel-fiber reinforced concrete, where the main parameters were the volumetric ratios of steel-fibers: 0.0, 0.5 and 1.0 percent. The cross section analytical model of PreSFC beam proposed in this study predicts the test results of behavior, strength and stiffness closely.

Keywords: Prestressed Concrete, Beam, SFRC, Cross Section Analysis, Flexural Strength, Initial Flexural Stiffness

INTRODUCTIONS

Steel-Fiber Reinforced Concrete (hereafter referred to SFRC) material has been developed and studied for application to structural members such as coupling beams and seismic walls. A property of SFRC is the pseudo strain hardening behavior caused by the distribution of multiple fine cracks under tensile stress.¹⁻³ Steel-fibers have been used to enhance tensile characteristics of concrete by suppressing crack growth and improving mechanical behavior.⁴ Concrete with steel-fibers is characterized by its steel-fiber content. The steel-fiber content is the weight of fibers per unit volume in concrete. It is the product of the volume fraction V_f (volume of fibers per unit volume of concrete, %) and the specific gravity of the fibers. It is still uncertain how the tensile characteristics of SFRC affect the flexural resistance mechanism of structural elements². Various analytical and empirical methods have been proposed to predict the flexural strength of the composite material reinforced with fibers.⁵⁻⁷ Of all the steel-fibers currently in use to reinforce cement matrices, steel-fibers are the only fibers that can be used for carrying long-term load.^{5, 8}

Prestressed concrete member requires the concrete to attain high compressive strength at an early stage to apply prestressing force. In addition to its higher compressive strength, high strength concrete possesses an increased tensile strength and reduced shrinkage and creep strains than normal concrete. High strength concrete has been found, however, to be more brittle when compared to normal strength concrete. Inclusion of fibers is one way to alleviate the problem of brittleness of high strength concrete. Pretensioned concrete members have been used to control crack width and deflection under service load. Prestressing force applied on them is generally smaller than the one of post tensioned members and pretensioned members do not need anchorage devices.

Addition of steel-fibers has been shown to increase flexural strength and ductility of structures made of prestressed concrete with normal concrete. Therefore, using steel-fiber reinforced concrete to prestressed concrete members (hereafter referred to PreSFRC), are expected to improve the toughness, the energy dissipation capacity, and the failure mode of pre-tensioned members. **Table 1** summarizes the advantages and disadvantages of SFRC and prestressed members.⁷ In order to overcome each disadvantage the synergy between SFRC and prestressing is expected to be one of the solutions under earthquake load. The present paper reports the influence of the steel-fiber reinforced concrete on the seismic behavior of prestressed concrete beam members

Table 1 Advantages and disadvantages of SFRC and prestressed member⁷

	Advantages	Disadvantages
SFRC	Smaller crack width, enhancing durability, More ductile	Constructability, Cost
Prestressed member	Smaller residual deformation, Smaller crack width	Brittle failure in compressed concrete

under earthquake load. For the rational design of a concrete structure, the complete stress-strain relationship of its constituent materials must be determined. Several material models have been proposed for normal concrete and steel-fiber reinforced concrete.⁹⁻¹⁴ However, the proposed models are too complicated to be adopted in practice. For example, since the concrete kinetic property changes with the shape and strength of steel-fiber, it is difficult to apply the influence of steel-fiber reinforced concrete with a same method. This is because of the difficulty in clearly understanding the complex flexural transfer mechanism. Moreover, a few research studies have been carried out to examine the role of fibers in the area of prestressed concrete applications and very few researches have been reported in the literature that have used the concept of inclusion of fibers over a partial depth of the beam member in the area of normal concrete without steel-fiber.⁸

REVIEW OF PREVIOUS RESEARCHES

Many studies have been conducted to clarify the flexural strength enhancement of SFRC members¹⁻²², most of them were concerned with the estimation of flexural strength based on empirical methods. A few researchers have been discussed the expressions for the compressive model of SFRC, the flexural strength of SFRC and the ultimate shear strength of PreSFC.⁸⁻²¹

Compressive Stress-Strain Behavior of SFRC by C. T. T. Hsu¹³

The main objective of C. T. T. Hsu research was to develop practical formulations based on the parameters of the complete stress-strain curve for high-strength concretes. The expression for stress-strain relationship under uniaxial compression can be represented by the following equations.

$$\eta = \frac{n \cdot \beta \cdot x}{n \cdot \beta - 1 + x_d n \beta} \quad \text{Eq. (1)}$$

where, $n = f_c / f'_c$, $x = \epsilon / \epsilon_0$, $\beta = 1 / (1 - (f'_c / (\epsilon_0 \cdot E_{ii})))$ for $\beta \geq 0$, β ; depends on the shape of the stress-strain diagram, n ; depends on the strength of material, η ; the normalized stress, x ; the normalized strain, f_c ; the stress in general, f'_c ; the peak stress of concrete, ϵ_0 ; strain corresponding to the peak stress, x_d ; the strain at $0.6f'_c$ in the descending portion of the stress-strain curve. **Fig. 1** shows the complete stress-strain curves for high-strength fiber reinforced concrete with the compressive strength of 11.98 ksi and fiber volume fraction of 1.0 percent at different volumetric ratios, which are generated by the present analytical equations for high-strength fiber reinforced concrete by Hsu. For example, n , β and ϵ_0 can be related to the compressive strength f'_c . The reason that f'_c is used to estimate the other parameters is that only the specified compressive strength is known during the design stages of most structures.

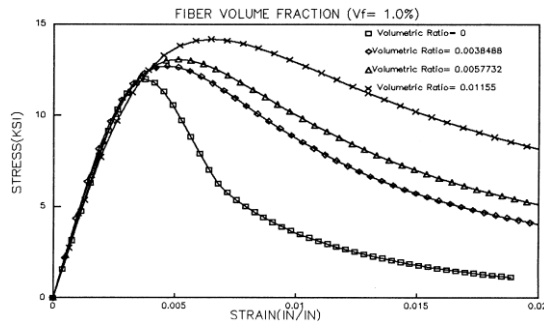


Fig. 1 Analytical stress-strain curves by Hsu¹³

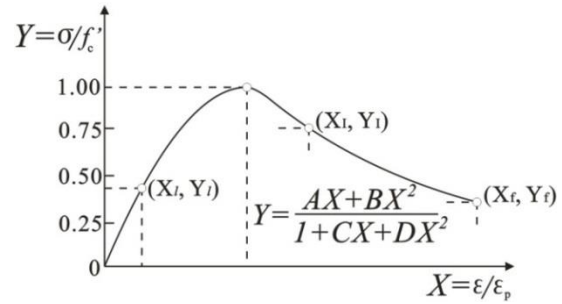


Fig. 2 Analytical compressive model of SFRC by Naaman¹⁴

Compressive Model of SFRC by Naaman¹⁴

The main objective of research by Naaman was to provide a comprehensive experimental and analytical evaluation of the stress-strain properties of fiber reinforced concrete in compression. The effects of the fiber reinforcing parameters are systemically investigated. **Fig. 2** shows the analytical compressive model of steel-fiber reinforced concrete by Naaman.¹⁴ To model various descending branches of the curve for the same ascending branch, different sets of constants A , B , C and D are used for each branch. The constants are determined from the boundary conditions. Based on the results of previous experiments and probabilistic analysis, Naaman defined compressive strength f'_c as shown in Eq. (2).

$$Y = \frac{AX + BX^2}{1 + CX + DX^2} \tag{Eq. (2)}$$

where, $X = \varepsilon/\varepsilon_p$; $Y = \sigma/f'_{cf}$; ε = strain in general; ε_p = strain at peak stress; σ = stress in general; f'_{cf} = peak stress of fiber reinforced matrix; A , B , C , D = constant to be determined from the boundary conditions of the curve.

Compressive Stress-Strain Curve by M. C. Nataraja²⁰

In the research by Nataraja, an extensive experimental work has been carried out to study the stress-strain behavior of steel-fiber reinforced concrete with compressive strength ranging from 30 to 50 N/mm². Three fiber volume fractions, 0.5%, 0.75% and 1.0%, and two aspect ratios, $l/d=55$ and 82, were studied. The influence of fiber addition on peak stress and strain at peak stress, the toughness of concrete and the nature of the stress-strain curve were investigated. Eq. (3) shows the proposed compressive model of SFRC by Nataraja.²⁰

$$\frac{f_c}{f'_{cf}} = \frac{\beta(\varepsilon_c/\varepsilon_{of})}{\beta - 1 + (\varepsilon_c/\varepsilon_{of})^\beta} \tag{Eq. (3)}$$

where, f'_{cf} ; the compressive strength of fiber concrete, ε_{of} ; the corresponding peak strain,

f_c, ϵ_c ; the stress and strain values on the curve, β ; the material parameter that depends on the shape of the stress-strain diagram.

To use Eq. (3) to generate the stress-strain curve for a given value of compressive strength of fiber concrete, f'_{cf} , only the value of ϵ_{of} and β are needed. It has been noticed in the present experimental investigation and by other researchers that fibers have more effective contribution on the compressive stress-strain curves in the descending branch. Therefore, using the experimental results, a best fitting statistical analysis was performed to obtain a relationship between the parameter β and the reinforcing index ($=w_f \times l/d$), of the fiber-reinforced concrete based on the physical property of the stress-strain curve, which is the slope of the inflection point at the descending segment as shown in Fig. 3.

Tensile Model of SFRC by Nanni²²

Among many reported tensile model of SFRC^{5, 6, 22} Antonio Nanni concept²², is introduced in this study, representatively. Fig. 4 shows the load-deformation curves for specimens with deformed-end fiber type B by Nanni. Nanni was considering any static tensile-type test for fiber reinforced concrete (hereafter referred to FRC) composites, there were three parameters of interest, i.e. first crack strength, ultimate strength and toughness. Nanni conducted the splitting-tension test for obtained the load-deformation relationships by type of steel-fiber and the volume fraction of fibers. From this test, the characteristic parameters of FRC subjected to tension were derived. It was concluded that the splitting-tension test adequately describes the performance of fiber reinforced concrete.

Tensile Model of SFRC by Swamy⁵

Fig. 5 shows the basic stress-strain relationship of SFRC by Swamy.⁵ Swamy employed the law of mixtures and took into account a random distribution factor, bond stress, fiber stress, and change in neutral axis resulting from nonlinear stress distribution.

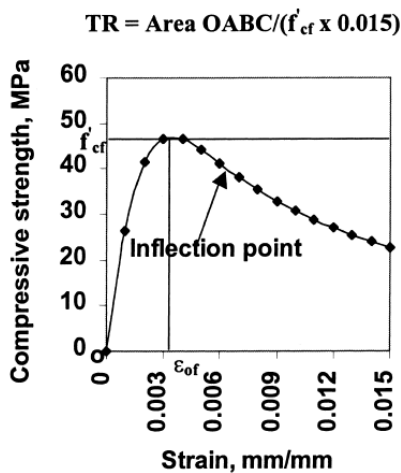


Fig. 3 Toughness ratio definition by Nataraja²⁰

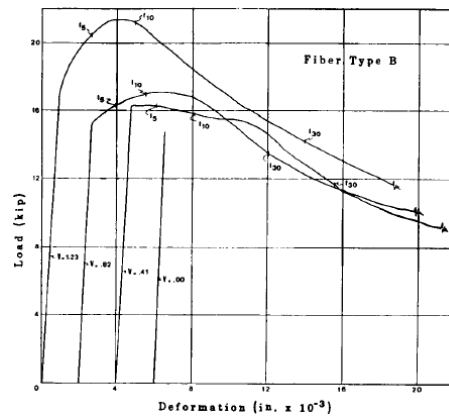


Fig. 4 Load-deformation curves of fiber type B by Nanni²²

As shown in **Fig. 5**, the basic design assumptions of SFRC were based on the CIP code. The following assumptions at tensile side are made for the analysis method by Swamy.

<Assumptions>

1. The height e of the elastic uncracked zone of concrete is very small compared to the neutral axis depth and it is therefore assumed that the tensile contribution of the steel-fibers is represented by a rectangular stress block over the whole of the tension zone of the beam.
2. The maximum usable strain at the extreme concrete compression fiber is 0.0035.

Tensile Model of SFRC by Henager⁶

Henager considered the tensile resistance ability of the cross section as shown in **Fig. 6**. The difference between Swamy and Henager is a depth of neutral axis at tensile side. Henager presented an analytical method to predict the flexural strength of steel-fiber concrete beams with bar reinforcement in which the bond stress, fiber stress, fiber aspect ratio, and volume fraction of fibers were taken into account. The following assumptions at tensile side are made for the analysis method by Henager.⁶

<Assumptions>

1. The tensile contribution of the steel-fibers is represented by a tensile stress block equal to the force required to develop the dynamic bond stress of the fibers that are effective in that portion of the beam cross section.
2. The tension is taken as the area with a minimum tensile strain of σ_f/E_s .

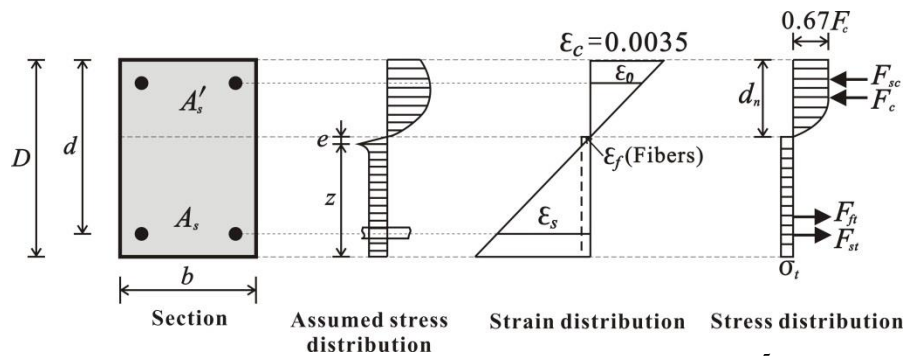


Fig. 5 Basic stress-strain relationship by Swamy⁵

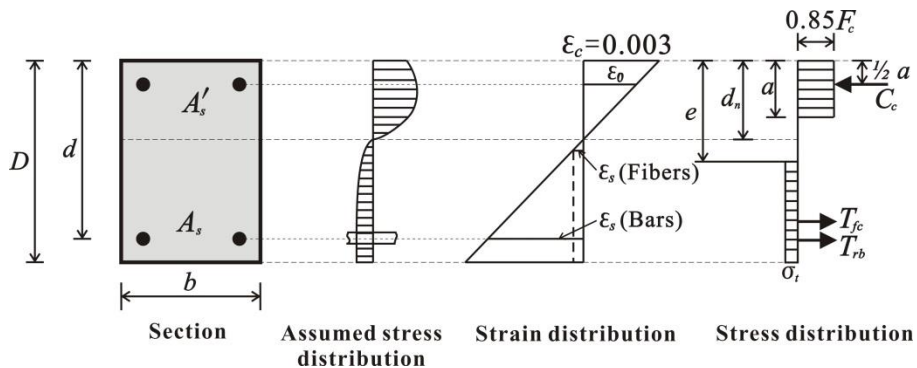


Fig. 6 Tensile stress-strain relationship by Henager⁶

CROSS SECTION ANALYSIS OF PRESFC BEAM

The main objective of this research was to propose a cross section analysis of PreSFC beam members, containing certain volume fraction of steel-fibers as follows; $V_f=0.0, 0.5, \text{ and } 1.0$ percent. The properties of steel-fibers are the diameter of 0.62 mm , length of 30 mm , and tensile strength of $1,200 \text{ N/mm}^2$.

Proposal Compressive Models of SFRC

Several material modellings for high-performance fiber reinforced cementations composite, HPRC, have been proposed to predict the flexural strength of fiber reinforced concrete members, i.e. beam and column, without prestressed.¹⁵⁻¹⁸ These models are not taking into account the fiber reinforced concrete such like the material used in this study.

The concrete of this study contained the aggregates of maximum diameter of 20 mm . The proposed concrete model has revised the Nakatsuka model^{19,20} (hereafter referred to *N* model) as shown in **Fig. 7**. *N* model was expressed with an ascending and decline areas. **Table 2** summarizes the formulas of *N* model.¹⁹ The *N* model was adopted for PreSFC cross section analysis so as to clarify why the *N* model was separated with an ascending and descending region, as shown in **Fig. 7**. By using steel-fiber reinforced concrete, the resistance capacity of tensile side will be enhanced. By the difference of volume fraction of steel-fibers, this study controlled a peak strain, ϵ_{peak} , and ultimate strain, ϵ_{ult} , when reached the maximum compressive strength, f'_c , and decreased the 50 percent of the maximum compressive strength as shown in **Fig. 8**. Moreover, the gradient after the maximum compressive strength, θ , by the volume fraction of steel-fibers was monitored and controlled in this study. **Fig. 9** shows the examples of theoretical compressive stress-strain relationships by volume fraction of steel-fibers, $V_f=0.0, 0.5, \text{ and } 1.0\%$ using the proposal model in this study. Therefore, this study was considering on the enhancement of tensile resistance capability of cross section.

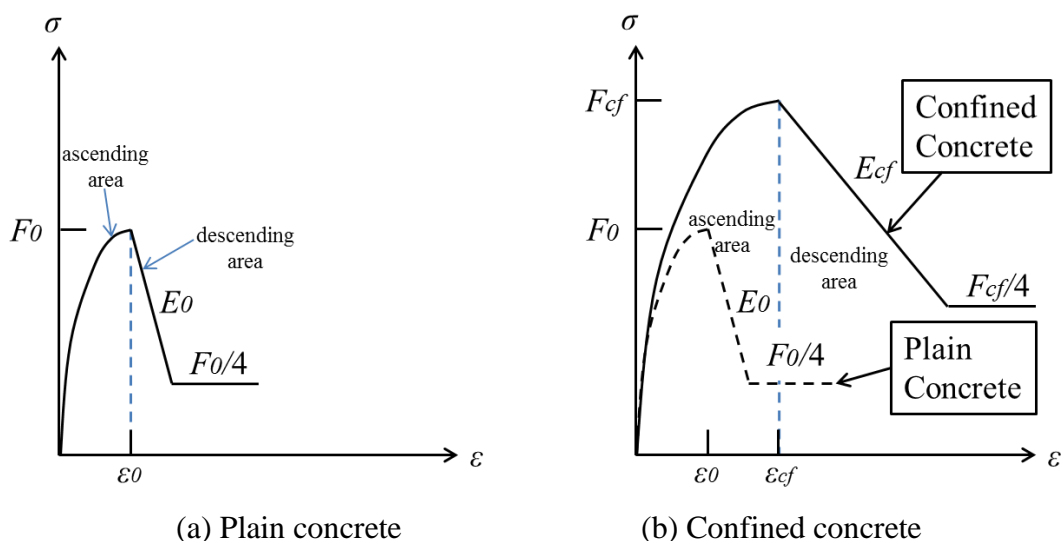


Fig. 7 Concept of *N* model¹⁹

Table 2 Summary of the *N* model¹⁹

	Plain Concrete	Confined Concrete
Ascending area	$\sigma_c = F_0 \left\{ 1 - \left(1 - \frac{\varepsilon_c}{\varepsilon_0} \right)^2 \right\}$ Eq. (4)	$\sigma_c = F_{cf} \left\{ 1 - \left(1 - \frac{\varepsilon_c}{\varepsilon_{cf}} \right)^n \right\}$ Eq. (6)
Descending area	$\sigma_c = F_0 \left\{ 1 - t_{\theta,0} \left(\frac{\varepsilon_c}{\varepsilon_0} - 1 \right) \right\}$ Eq. (5)	$\sigma_c = F_{cf} \left\{ 1 - t_{\theta,cf} \left(\frac{\varepsilon_c}{\varepsilon_{cf}} - 1 \right) \right\}$ Eq. (7)

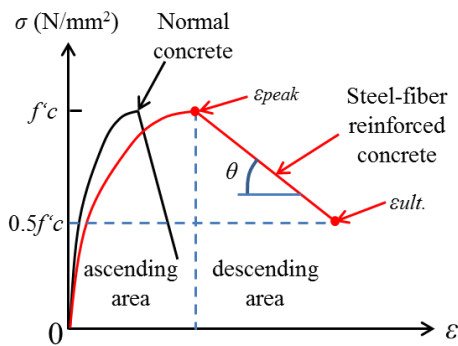


Fig. 8 Concept of compressive model of SFRC

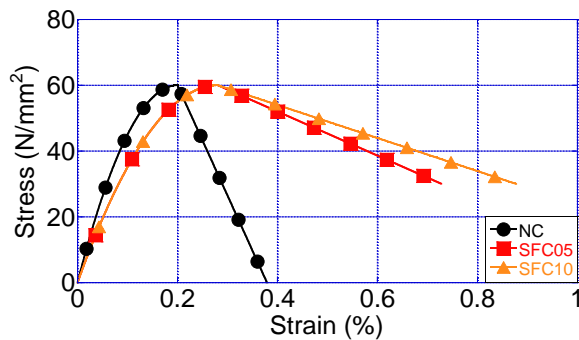


Fig. 9 Theoretical compressive stress-strain curves by volume fraction of steel-fibers

Table 3 summarizes the proposal compressive model of SFRC. In this study, parameter α was introduced into the *N* model to model the gradient θ in the descending area, as shown in Eq. (9) and Eq. (11). In the cross section analysis, the concrete areas outside and inside the stirrups were defined as plain and confined concrete, respectively. **Table 4** shows the summary of ε_{peak} , ε_{ult} , and α based on the test results.

Table 3 Summary of the proposal compressive model of SFRC

	Plain Concrete	Confined Concrete
Ascending area	$\sigma_c = F_0 \left\{ 1 - \left(1 - \frac{\varepsilon_c}{\varepsilon_0} \right)^2 \right\}$ Eq.(8)	$\sigma_c = F_{cf} \left\{ 1 - \left(1 - \frac{\varepsilon_c}{\varepsilon_{cf}} \right)^n \right\}$ Eq.(10)
Descending area	$\sigma_c = F_0 \left\{ 1 - \alpha^{*1} t_{\theta,0} \left(\frac{\varepsilon_c}{\varepsilon_0} - 1 \right) \right\}$ Eq.(9)	$\sigma_c = F_{cf} \left\{ 1 - \alpha^{*1} t_{\theta,cf} \left(\frac{\varepsilon_c}{\varepsilon_{cf}} - 1 \right) \right\}$ Eq.(11)

*1: the factor of decline gradient (≤ 1.0 , *N* model is 1.0)

Table 4 Summary of ϵ_{peak} , $\epsilon_{ult.}$ and α of proposal model

V_f^{*1} (%)	ϵ_{peak}^{*2}	$\epsilon_{ult.}^{*3}$	α^{*4}
0.0	0.259	0.200	1.00
0.5	0.281	0.695	0.20
1.0	0.281	0.849	0.15

*1: volume fraction of fibers, *2: strain at reached the peak splitting tensile strength, *3: strain at the strength reduced to 50% of f'_c , *4: the factor of decline gradient (≤ 1.0 , N model is 1.0)

Proposal Tensile Models of SFRC

The splitting tensile model of SFRC by volume fraction of steel-fiber reinforced concrete controls the ultimate strain when it reaches the ultimate state. That is because unlike the ultimate strain, there was no significant difference of the maximum splitting tensile strength when the volume fraction of steel-fibers varied.

Fig. 10 shows the concept of splitting tensile strength model of SFRC. **Fig. 11** shows the tensile stress-strain relationship of the proposal model in this research. **Table 5** shows the summary of the proposal tensile model of SFRC.

Hysteresis Model of Concrete, Rebar and PC Strand

Fig. 12, **Fig. 13** and **Fig. 14** show the hysteresis model of each material used in this study, i.e. concrete, rebar and PC strand. The hysteresis model of rebar is *Okada-Muguruma* model based on *Ramberg-Osgood* method.²⁷ The PC strand hysteresis model is a tri-linear model in accordance with Architectural Institute of Japan.²⁸

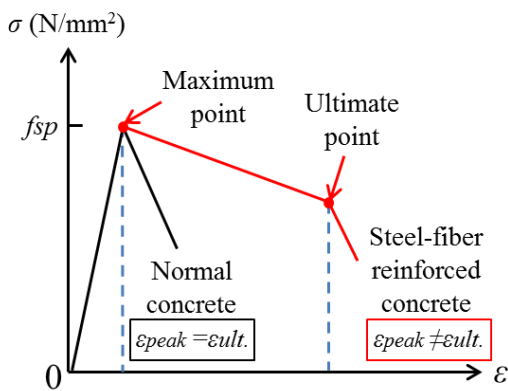


Fig. 10 Concept of tensile model of SFRC

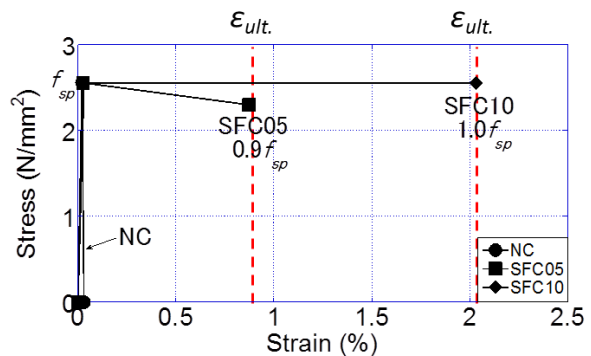


Fig. 11 Proposal tensile model of SFRC

Table 5 Summary of proposal tensile model in this research

V_f^{*1} (%)	At the maximum		At the ultimate	
	σ (N/mm ²)	ϵ_{peak}^{*2}	σ (N/mm ²)	$\epsilon_{ult.}$
0.0	f_{sp}	0.020	0.0	0.020
0.5	f_{sp}	0.026	$0.9 f_{sp}$	0.873
1.0	f_{sp}	0.031	$1.0 f_{sp}$	2.031

*1: volume fraction of fibers, *2: strain at the maximum load

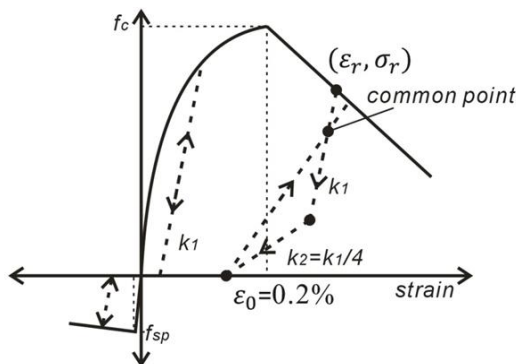


Fig. 12 Hysteresis model of concrete²⁶

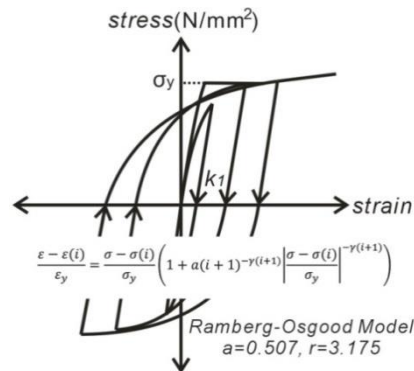


Fig. 13 Hysteresis model of rebar²⁷

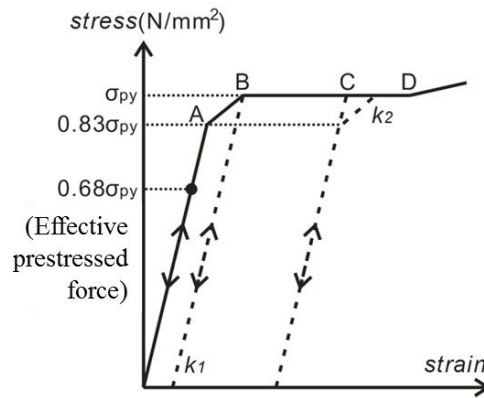


Fig. 14 Hysteresis model of PC strand²⁸

Flow of Cross Section Analysis

Fig. 15 shows the flow of the cross section analysis. The assumption of *Navier Hypothesis* was considered in the analysis. The tensile resistance effect by steel-fibers was considered, as well. Moreover, the inelastic hinge length was 1.0D. **Fig. 16** shows the displacement control rule for cross section analysis.

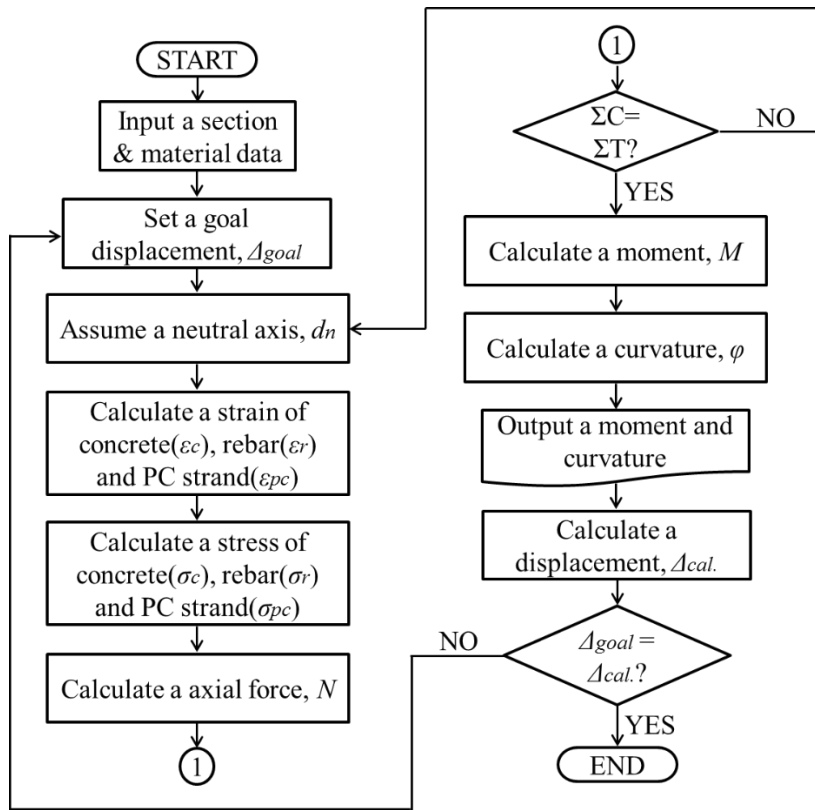


Fig. 15 Flow of cross section analysis

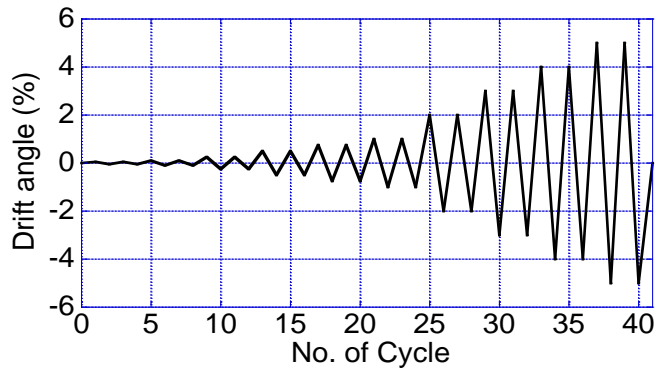


Fig. 16 Displacement control plan for analysis

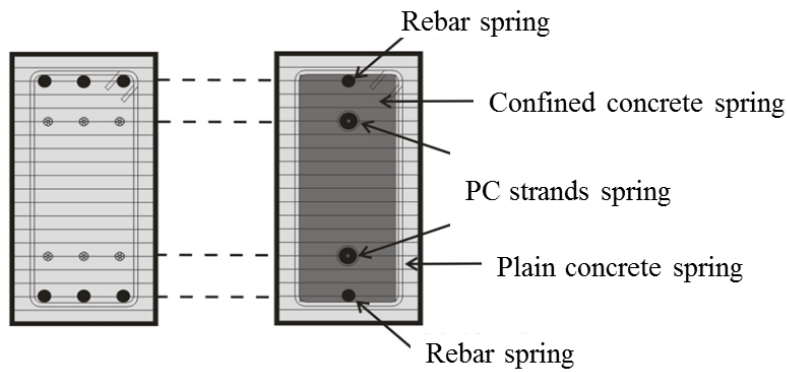


Fig. 17 Cross section for analysis

Fig. 17 shows the cross section and its simplification for the analysis.. The bars and the PC strands were modelled as springs and located at the vertical centerline of the cross section.

ANALYSIS RESULTS AND DISCUSSIONS

Shear Force-Drift Angle Relationships

Fig. 18 shows the shear force-drift angle curves for all specimens. The test results, PC3-test, PC3-SF05-test and PC3-SF10-test, in **Fig. 18** are the results of anti-symmetric test from **References 24** and **25**. The cross section analysis of the PreSFC was carried out to predict the flexural deformation. Therefore, **Fig. 18** only shows the flexural deformations of the experiment results. PC3 specimen, $V_f=0.0\%$, adopted the original *N* model. A good agreement between the test and the analysis results can be seen in the figure. Especially, the maximum flexural strengths of PC3 and PC3-SF05 show the almost same strength and drift angle.

The Maximum Flexural Strength

Table 9 compares the results for the shear force. The error ratios of maximum flexural strength of PC3 ($V_f=0.0\%$) were 4.0% in (+) side and 6.4% in (-) side used *N* model and did not considered tensile resistance by concrete. As a results, PC3 specimen, $V_f=0.0\%$, could evaluated very closely using original *N* model.

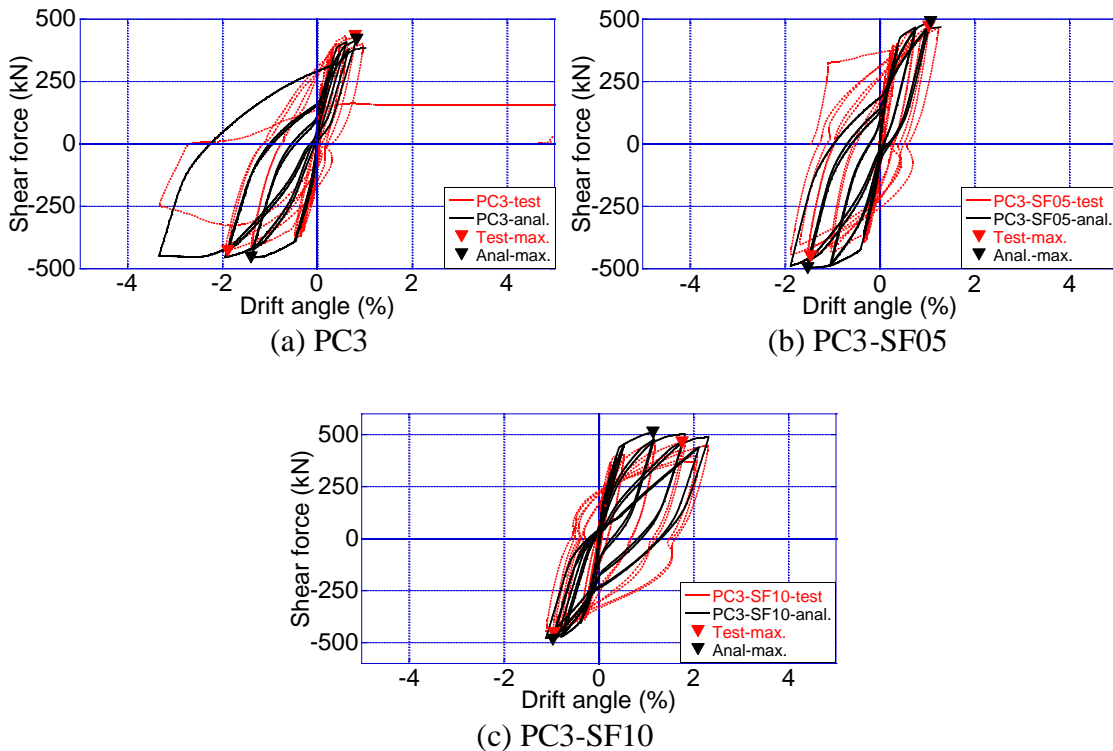


Fig. 18 Shear force-drift angle relationships

Table 9 Comparison of maximum strength

Specimens	$test Q^{*1}$ (kN)		$anal. Q^{*2}$ (kN)		$anal. Q / test Q$ (%)	
	(+)	(-)	(+)	(-)	(+)	(-)
PC3 ($V_f=0.0\%$)	432.9	428.6	415.5	456.0	96.0	106.4
PC3-SF05 ($V_f=0.5\%$)	470.3	450.2	488.5	497.5	103.9	110.5
PC3-SF10 ($V_f=1.0\%$)	462.9	452.9	510.6	485.5	110.3	107.2

*1: test results from reference 24, *2: analysis results by proposal model in this research

The error ratios of PC3-SF05 ($V_f=0.5\%$) and PC3-SF10 ($V_f=1.0\%$) varied between 3.9 to 10.5% when the proposal model was implemented. Moreover, the drift angles of PC3-SF05 specimen at the maximum flexural strength were very close to test results as shown in **Fig. 18**. The drift angle of the (+) side of PC3-SF10-test at the maximum flexural strength shows the one cycle after.

Initial Flexural Stiffness

Table 10 shows the derived stiffness based on the experiment works and the analysis. In this study, the initial flexural stiffness was calculated by Eq. (12) and Eq. (13).

$$M = EI \cdot \varphi \quad \text{Eq. (12)}$$

$$K_b = \frac{EI}{L^3} \quad \text{Eq. (13)}$$

where, M ; moment from analysis (kN·m), E ; Young's modulus of concrete (N/mm²), I ; inertia moment of cross section (mm⁴), φ ; curvature (mm⁻¹), K_b ; initial flexural stiffness (kN/mm), L ; length of specimen (mm).

The Young's modulus, E , was acquired from the concrete cylinder compressive tests.

A curvature, φ , from test results was calculated using the LVDTs as shown in **Fig. 19**. It can be seen that the analytical initial flexural stiffness of PC3, $V_f=0.0\%$, was 5.8% larger than the test result.

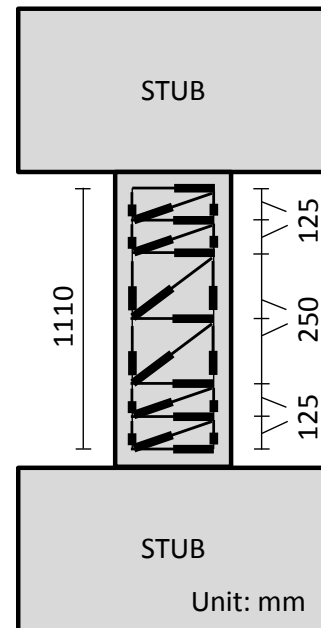
**Fig. 19** Location of LVDTs

Table 10 Comparison of initial flexural stiffness

Specimens	Test	Analysis	$\frac{\text{anal.}K_b}{\text{test}K_b}$ (%)
	$\text{test}K_b^{*1}$ (kN/mm)	$\text{anal.}K_b^{*2}$ (kN/mm)	
PC3 ($V_f=0.0\%$)	305.6	323.3	105.8
PC3-SF05 ($V_f=0.5\%$)	393.8	378.6	96.1
PC3-SF10 ($V_f=1.0\%$)	424.8	386.5	91.0

*1: the initial flexural stiffness of test results from reference 24, *2: the initial flexural stiffness of cross section analysis in this research

The error ratios of PC3-SF05 and PC3-SF10 specimens were 3.9 and 9.0% to the test results, as shown in **Table 10**. The proposed model could predict the initial flexural stiffness of PreSFC beam member within 9.0% error.

CONCLUSIONS

The following conclusions were drawn from the results of this research.

- 1) The cross section analytical results of PC3 ($V_f=0.0\%$) and PC3-SF05 ($V_f=0.5\%$) specimens not to exceed about 4.0% on the maximum flexural strength; and 6.0% on the initial flexural stiffness.
- 2) The error ratios of maximum flexural strength of PC3-SF05 and PC3-SF10 varied between 3.9 to 10.5% when the proposal model was implemented. Moreover, the drift angles of PC3-SF05 specimen at the maximum flexural strength were very close to test results.
- 3) The errors of initial stiffness of PC3-SF05 and PC3-SF10 specimens were 3.9 and 9.0% to the test results. The proposed model could predict the initial flexural stiffness of PreSFC beam member within 9.0% error.

ACKNOWLEDGMENT

This research was supported by JSPS KAKENHI Grant Number 24·5797.

I wish to sincerely appreciate Prof. Minehiro NISHIYAMA for his excellent ideas and constant supervisory during my doctoral course at Kyoto University.

REFERENCES

1. Minoru Kunieda, Keitetsu Rokugo, "Recent progress on HPFRCC in Japan", *Journal of Advanced Concrete Technology, JCI*, Vol. 4, No.1, 19-33, 2006.
2. Haruhiko Suwada, Hiroshi Fukuyama, "Experimental and analytical study on influencing factors on shear strength and deformation capacity of damper using high performance fiber reinforced cementitious composite", *J. Struct. Constr. Eng., AIJ*, No.612, 171-178, 2009. (in Japanese)
3. Haruhiko Suwada, Hiroshi Fukuyama, "Noliner finite element analysis on shear failure of structural elements using high performance fiber reinforced cement compsite", *Journal of Advanced Concrete Technology, JCI*, Vol. 4, No.1, 45-57, 2006.
4. Bilal S. Hamad, Mohamad H. Harajli, and Ghaida' Juma, "Effect of fiber reinforcement on bond strength of tension lap splices in high-strength concrete", *Structural Journal, ACI*, Vol. 78, No.36, 395-405, 2001.
5. R. N. Swamy, Sa'ad A. Al-Ta'an, "Deformation and ultimate strength in flexural of reinforced concrete beams made with steel fiber concrete", *Structural Journal, ACI*, Vol. 78, No.36, 395-405, 1981.
6. Charles H. Henager, M. ASCE and Terrance J. Doherty, "Analysis of reinforced fibrous concrete beams", *Journal of Structural Division, ASCE*, Vol. 102, No.ST1, 177-188, 1976.
7. Hyeong Jae YOON, Minehiro NISHIYAMA, "Behavior of Pretensioned Concrete Beams Using Steel-fiber Reinforced Concrete", 15th World Conference of Earthquake Engineering, Lisbon, Portugal, 2012.
8. S. K. Padmarajaiah and Ananth Ramaswamy, "Behavior of fiber-reinforced prestressed and reinforced high-strength concrete beams subjected to shear", *Structural Journal, ACI*, Vol. 98, No.5, 752-761, 2001.
9. Ahmad S. H. and Shah S. P., "Stress - Strain Curve of Concrete Confined by Spiral Reinforcement", *ACI Journal, Proceedings*, Vol. 79, No. 6, Jan.-Feb., 484-490, 1982.
10. Carreira D. J. and Chu K. H., "Stress - Strain Relationship for Plain Concrete in Compression", *ACI Journal, Proceedings*, Vol. 82, No. 6, Nov.-Dec., 797-804, 1985.
11. Kent D. C. and Park K., "Flexural Members with Confined concrete", *Journal of the Structural Division, ASCE*, ST. 7, July, 1969-1974, 1971.
12. Minoru Kunieda, Keitetsu Rokugo, "Recent progress on HPFRCC in Japan", *Journal of Advanced Concrete Technology, JCI*, Vol. 4, No.1, 19-33, 2006.
13. Lin Showmay Hsu and Cheng-Tzu Thomas Hsu, "Stress-Strain Behavior of Steel-Fiber High Strength Concrete under Compression", *ACI Structural Journal*, Vol. 91, No. 4, Jul.-Aug., 448-457, 1994.
14. Fanella D. A. and Naaman A. E., "Stress-Strain Properties of Fiber Reinforced Mortar in Compression", *ACI Journal, Proceedings*, Vol. 82, No. 3, May-Jun., 475-482, 1985.
15. Antonie E. Naaman, "Engineered Steel Fibers with Optimal Properties for Reinforcement of Cement Composites", *Journal of Advanced Concrete Technology*, Vol. 1, No. 3, pp.241-252, Nov., 2003.
16. David A. Fanella and Antonie E. Naaman, "Stress-Strain Properties of Fiber Reinforced Mortar in Compression", *ACI Journal*, Vol. 82, No. 4, pp.475-483, July-August, 1985.
17. T. Y. Lim, P. Paramasivam, and S. L. Lee, "Analytical Model for Tensile Behavior of

- Steel-Fiber Concrete”, *ACI Material Journal*, Vol. 84, No. 4, pp.286-298, July-August, 1987.
18. H. C. Lima, Jr. and J. S. Giongo, “Theoretical Model for Confined Steel-Fiber Reinforced High-Strength Concrete”, *ACI Special Publication*, Vol. 229, pp.273-286, September 1, 2005.
 19. Tadashi Nakatsuka, “Research of Concrete Stress-Strain Characteristics and Ultimate Area Characteristics on Concrete Flexural Member”, Ph.D. Thesis, Osaka University, 1991. (in Japanese)
 20. M. C. Nataraja, N. Dhang and A. P. Gupta, “Stress-strain curves for steel-fiber reinforced concrete under compression”, *Cement & Concrete Composites* 21, pp.383-390, 1999.
 21. P. A. Jones, S. A. Austin and P. J. Robins, “Predicting the flexural load-deflection response of steel fibre reinforced concrete from strain, crack-width, fibre pull-out and distribution data”, *Materials and Structures*, pp.449-463, 2008.
 22. Antonio Nanni, “Splitting-Tension Test for Fiber Reinforced Concrete”, *ACI Materials Journal*, Feb., 229-233, 1988.
 23. Japan Architecture Center, *Design and calculation example of Prestressed Concrete Technical Standard*, 2009. (in Japanese)
 24. Hyeong Jae YOON, “Seismic Performance of Prestressed Concrete Beams Using Steel-Fiber Reinforced Concrete”, Ph.D. Thesis, Kyoto University, 2014.
 25. Hyeong Jae YOON, “Seismic Performance of Precast PC Beams Using SFRC”, *Precast/Prestressed Concrete Institute*, 2014 PCI/NBC, 2014.
 26. Architectural Institute of Japan, “Design method of Prestressed Concrete Structural Member-Now and Future-”, 2000.
 27. Okada, Muguruma, “Handbook of Concrete Structure”, Asakurashoten, 1985.
 28. Architectural Institute of Japan, “Toughness Design Method and Application to Seismic Ramen of Concrete Structure (PC, PRC) Member”, 1997.